Editors' Suggestion

Hydrodynamic interaction leads to the accumulation of *Chlamydomonas reinhardtii* near a solid-liquid interface

Chunhe Li, Hongyi Bian, Yateng Qiao, Jin Zhu, and Zijie Qu, *

**UM-SJTU Joint Institute, Shanghai Jiao Tong University, Shanghai 200240, People's Republic of China



(Received 8 November 2024; accepted 2 April 2025; published 9 May 2025)

The physical mechanism of microbial motion near solid-liquid interfaces is crucial for understanding various biological phenomena and developing ecological applications. However, limited works have been conducted on the swimming behavior of *C. reinhardtii*, a typical "puller" type cell, near solid surfaces, particularly with varying and conflicting experimental observations. Here, we investigate the swimming behavior of *C. reinhardtii* using a three-dimensional real-time tracking microscopy system both near a solid-liquid interface and in the fluid bulk region. We explore the relationships between the cell density, swimming speed and orientation with respect to the distance from the solid-liquid interface, confirming the phenomenon of *C. reinhardtii* accumulation near the solid-liquid interface. Based on the traditional definitions of "pusher" and "puller" cells, we propose a simplified model consisting of a pair of mutually perpendicular force dipoles for *C. reinhardtii*. This model is employed to analyze the complex hydrodynamic interactions between *C. reinhardtii* and the solid surface, providing a potential theoretical explanation for the observed accumulation phenomenon at the solid-liquid interface.

DOI: 10.1103/PhysRevE.111.L052401

Introduction. Microogranisms achieve locomotion in fluidic environments using various strategies, including rotating rigid helical flagellum [1,2], beating flexible cilia [3,4], and constantly deforming their cell bodies [5,6], to conquer the time reversibility of the Stokes equation [7]. The flow fields generated by these creatures differ dramatically as a result of their swimming modes and are commonly classified as a pusher or puller type [8]. The difference between these types lies in the direction of flow along the axis of net swimming [9–11]. Understanding the hydrodynamic interaction between the self-propulsion cells and the ambient fluid is crucial in revealing the physical essence of many biological phenomena, such as the biofilm formation [12–14], the spread of intestinal diseases [15,16], and bacteria swarming [17,18]. Moreover, most of these processes occur near a fluid-solid interface. Thus, it is important to study the swimming behavior of microorganisms near solid surfaces.

In previous works, several physical mechanisms have been proposed to elucidate the cell-surface interaction including the wall scattering [19,20], steric interaction [16], and hydrodynamic interaction [21–23]. These interactions lead to surface accumulation and near-surface rotational motion of pusher-type cells, like bacterium *E. coli* and sperm [24–27]. Nevertheless, *Chlamydomonas reinhardtii*, a typical puller-type cell, has also been observed to accumulate near the solid surface. In one of the most recent works, Buchner *et al.* [28] used a 3D tracking microscope to investigate the hopping trajectory of *C. reinhardtii* near the solid surface and conclude that the accumulation is due to long-range interaction. However, the physical interpretation of such interaction remains unclear.

Here, we use a customized 3D tracking microscope that actively adjusts the focal plane and microscope stage in real time to investigate the swimming behavior of *C. reinhardtii* in an unconstrained chamber. Our experimental approach ensures long-term tracking with sufficient statistics for individual behavior analysis. Similar to the existing works, the surface accumulation of the cell and the hopping trajectory are both observed. A double force dipole model is developed to explain the hydrodynamic interaction between the cell and the surface which leads to the accumulation. The cell distribution in the observation chamber at the steady state is also well explained using a convection-diffusion model.

Result and discussion: C. reinhardtii accumulate near solid surface. To investigate the distribution of C. reinhardtii density at different distances from the solid-liquid interfaces, the cell suspension is injected in an observation chamber with a height of 700 µm (approximately 70 times the body length of the cell D [29], see Fig. 1). The other two dimensions of the chamber are approximately 1 cm, so the wall effect from the side is negligible. As shown in Fig. 1, cell suspension is observed on two occasions. One right after the cell suspension is put into the chamber (unsteady state), and the other one is when the cell density at different heights of the chamber no longer changes over time (steady state). From our measurement, the typical time for the system to reach the steady state is 30 min.

At the steady state, the number density of the cell is measured and depicted in Fig. 2. (Note: Percoll is added to the suspension to balance the effect of gravity [30]). z/D represents the distance between the cell in the chamber and the lower surface. A comparison between suspension with and without Percoll is shown in Fig. S1 in the Supplemental Material [31]. Obviously, the cell density is much higher near the top and bottom surfaces of the chamber than in the bulk region. Our result is similar to the one from Buchner *et al.*

^{*}Contact author: zijie.qu@sjtu.edu.cn

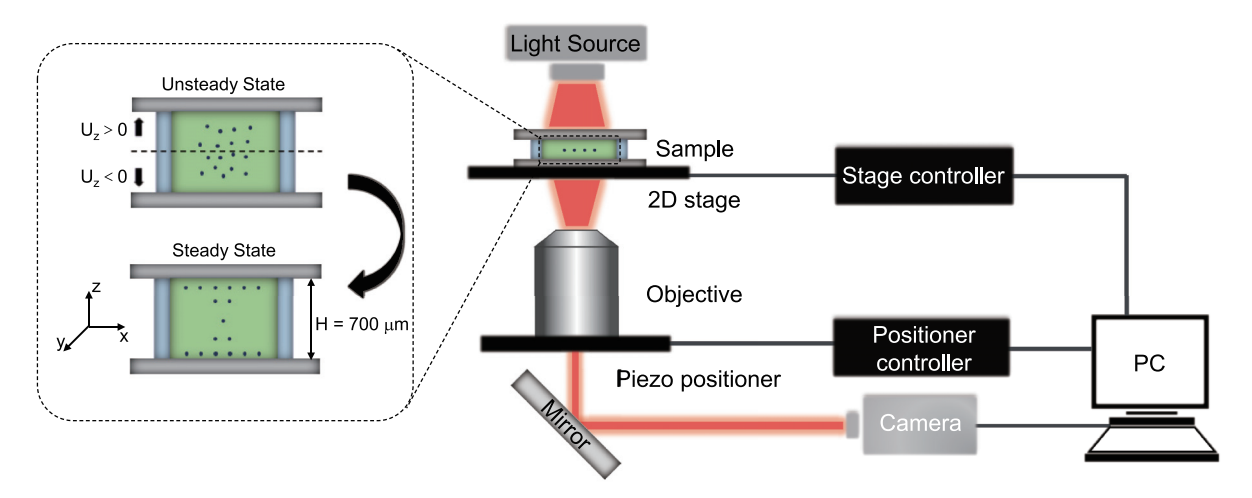


FIG. 1. Schematic of the experimental apparatus. The cell suspension is placed in a cylindrical chamber and illuminated under red light. Manually adjusting the *z*-axis height and capturing images to measure the distribution of cells at different distances from the wall. The microscope, duplicated from Qu *et al.*'s study [43], includes a stage controller and a positioner, which work together to record the 3D position of cells.

[28]. Notably, although *E. coli* and *C. reinhardtii* are known to swim very differently [32,33], the accumulation phenomenon observed here and in previous works [28] shows strong similarity to those studies focusing on *E. coli* cells [30,34]. It has been argued that the reason for *E. coli* being "trapped" is the hydrodynamic interaction between a pusher-type force dipole and a solid surface [29,35]. However, *C. reinhardtii* has been treated as a typical "puller-type" cell, which makes the accumulation phenomenon puzzling. In fact, it has been shown that *C. reinhardtii* is repelled from the hard surface either through a direct-contact mechanism [19] or a noncontact interaction [36].

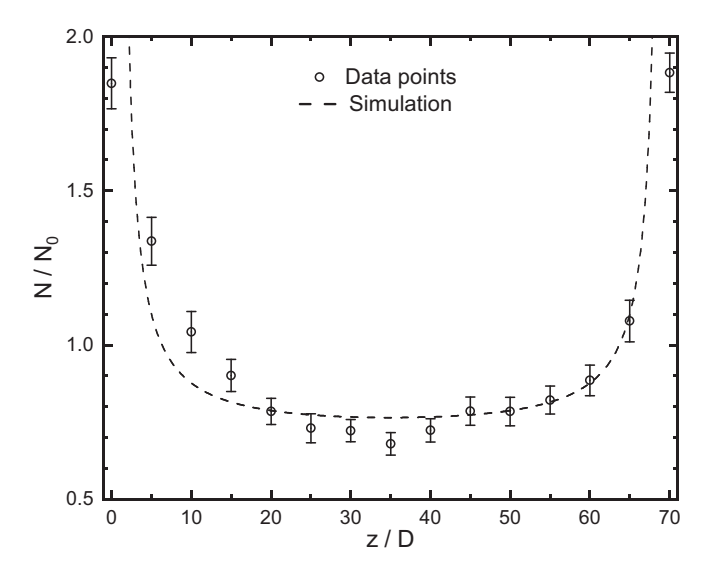


FIG. 2. Density distribution of *C. reinhardtii* at different distances from the solid-liquid interfaces. For each focal plane, three different regions are selected for cell counting, and the whole experiment is repeated five times. Data points indicate the measured distribution which can be expressed as a function of distances to the lower surface (z/D=0). The black dashed line, based on convection-diffusion simulation [30], fits the data points with $N_0=0.67$ and $L_0=23$ µm.

Swimming behavior near the surface. To fully understand the swimming behavior of C. reinhardtii, a three-dimensional real-time tracking microscope is developed (see Fig. 1) to follow individual cells over an extended period of time. Over 30 cells are tracked at different heights and the swimming behavior of each cell is recorded over 25 seconds (see Fig. S2 in the Supplemental Material [31]). First, we compare the swimming speed at three typical heights (z/D = 5, 35, 65) for both the steady and unsteady cases. As depicted in Figs. S4A and S4B in the Supplemental Material [31], the average swimming speed is almost the same. This indicates that neither the cell density nor the existence of the solid boundary influences the absolute swimming speed of the cell. Next, the vertical component of the velocity, U_z (velocity along the z axis) is averaged and shown in Fig. 3. Here, an interesting trend is found. In the unsteady state, U_z increases linearly with height and is close to zero in the middle of the chamber. This implies that the cell quickly migrates toward the solid boundary right after the suspension is injected. Such "attraction" scales linearly with distance. It is also worth noting that U_z is positive at the bottom surface and negative at the top, violating the overall trend. However, this can be well explained by the fact that the cell is bounced back from the surface as mentioned by different studies [19,37]. After the system evolves to the steady state, U_7 is close to zero at different heights (Fig. 3, black markers) except at the surfaces where the bouncing mechanism still exists.

Composite force dipoles hypothesis. Where does such "attraction" come from? Here, we propose a hypothesis that the hydrodynamic interaction between *C.reinhardtii* and the fluid is a combination of a simple "puller-type" force dipole and a "pusher-type" force dipole. As it has been previously studied, *C.reinhardtii* swims by periodically beating a pair of cilia [38,39]. The model that the cell is a "puller" roots in the fact that over one breaststroke cycle, the cell is being pulled by the cilia in front of it. However, during the initial part of this process, both cilia are swung to the side of the cell, exerting little pulling force on the cell body. This still introduces a strong interaction with the fluid and we believe

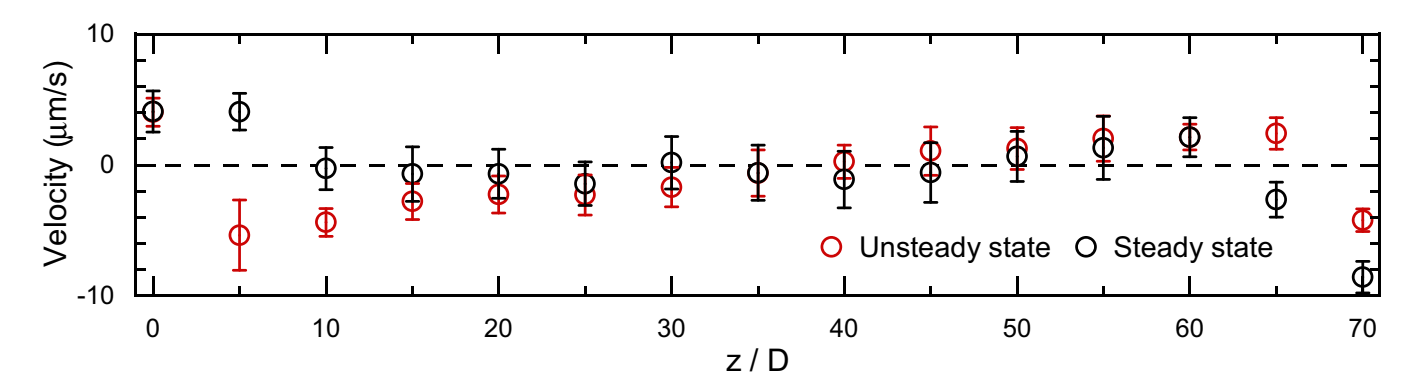


FIG. 3. z-velocity component of steady state cells (black points) and unsteady state cells (red points) at different distances from the solid-liquid interfaces. Each data point represents the trajectory of ten cells measured separately, with the error bar indicating the standard deviation of the mean velocities of different cells at the same location.

it can be treated as a "pusher-type" force dipole. The later part of the breaststroke cycle still introduces a "puller-type" interaction as it has been investigated for a long time [3,36].

We model *C.reinhardtii* as a pair of perpendicularly located "pusher" dipole, p_1 and a "puller", p_2 [see Fig. 4(a)]. Mathematically, the flow field induced by a Stokeslet dipole near a solid surface can be expressed as [30]

$$U_z(\theta_1, \theta_2, h) = -\frac{3}{64\pi \eta h^2} [p_1(1 - 3\sin^2\theta_1) - p_2(1 - 3\sin^2\theta_2)], \quad (1)$$

where p_i is the strength of the force dipole, θ_i and h are the angle and distance between the force dipole and the surface, and η is the fluid viscosity. Moreover, the strength of force dipole |p| scales as $\eta U L^2$ [40], where U is the cell swimming speed, and L is the characteristic length scale [17]. In our future analysis, we choose $U = 60 \,\mu\text{m/s}$ and $\eta = 2.98 \times 10^{-3} \,\text{Pa} \,\text{s}$. The swimming speed comes from our measurement and η is the viscosity of the buffer (see Fig. S4 in the Supplemental Material [31]) at room temperature.

Based on past research on cilia oscillations [41], we assume the cilia sweep through an area covered from -45° to 45° [shown in Fig. 4(b)] to generate most of the propulsion [42]. Deducing that the ratio of characteristic length scale between "pusher" and "puller" L_{p_1}/L_{p_2} is $(D_{\text{cell}} + 2 \times L_{\text{cilia}} \times \cos 45^{\circ})/(D_{\text{cell}} + L_{\text{cilia}} \times \cos 45^{\circ}) \approx 1.414$ (diameter of cell and length of cilia are both $10 \, \mu \text{m}$). Hence, the strength of p_1 is approximately twice greater than that of p_2 under the same cilia beating velocity.

With this assumption, we first calculate the flow field as a result of the two force dipoles using the equation

$$U(\mathbf{r}) = \frac{p_1 - p_2}{8\pi \eta r^3} [1 - 3\sin^2\theta]\mathbf{r}$$
 (2)

[shown in Fig. 4(c)]. The result is similar to the ones measured experimentally [9] and simulated [20]. Since we argue that this is a time-averaged result, some features such as the vortex of the flow field are missing when compared with the previous works. Next, we use Eq. (1) to investigate the velocity along the z axis as a function of θ_i . Due to symmetry, we only need to consider the case where the angle between the force dipole and the xy plane is within $(0, \pi/2)$, see a detailed description

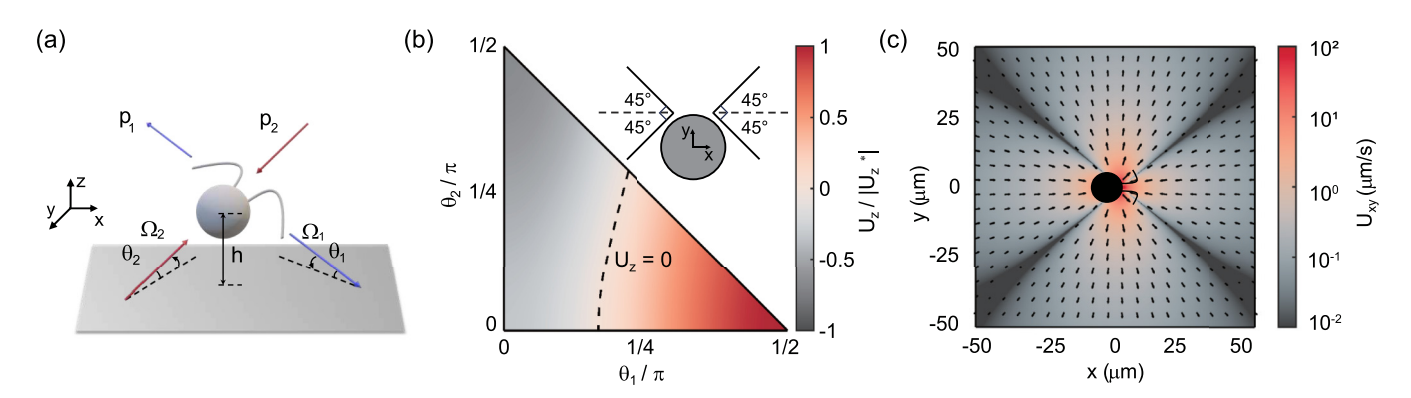


FIG. 4. (a) Schematic diagram illustrating the assumption of composite force dipoles. Force dipoles p_1 and p_2 are in a perpendicular configuration. p_1 behaves akin to a "pusher," while p_2 behaves akin to a "puller." The angle of p_1 and p_2 with respect to the plane and the angular velocity of rotation, when the distance of the cell from the wall is h. (b) Simplified depiction of C. reinhardtii swimming, with flagellar beating within a 90° range. Under the assumption of an aspect ratio of 1.414, variations in fluid velocity around the cell for different angles between the cell and the plane are illustrated. Color is normalized by the local velocity and the maximum magnitude of velocity. (c) xy-plane simulation velocity field near C. reinhardtii under the "pusher" and "puller" types. Arrow lengths and the color represent the logarithmic scaling of local velocity and maximum magnitude of velocity normalized.

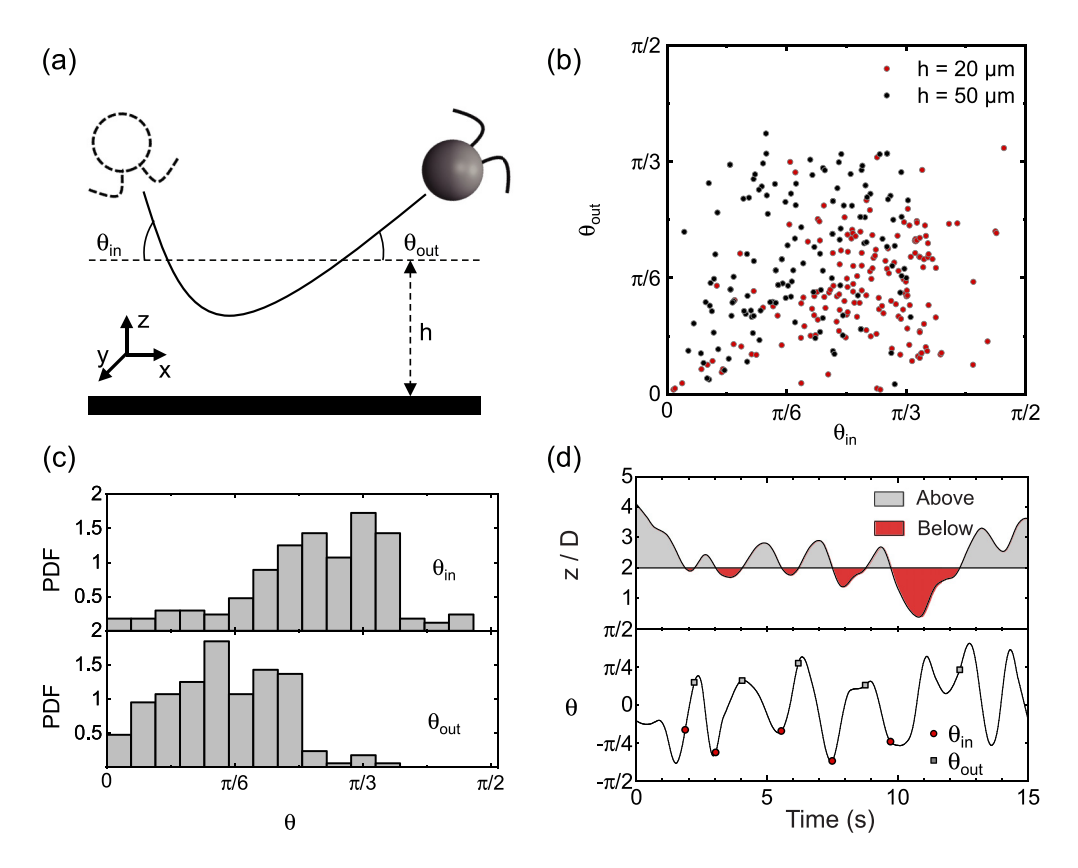


FIG. 5. (a) Schematic of the approaching and leaving angles of *C. reinhardtii* during swimming near the wall surface. (b) Distribution of $\theta_{\rm in}$ and $\theta_{\rm out}$ for *C. reinhardtii* away from $(h=50\,\mu{\rm m})$ and near $(h=20\,\mu{\rm m})$ the surface. (c) The histogram indicates that in the case of $h=20\,\mu{\rm m}$, approaching angles $\theta_{\rm in}$ are biased around $\pi/3$, while receding angles $\theta_{\rm out}$ are biased around $\pi/6$. (d) One typical cell swimming trajectory which has approached and left the surface $(h=20\,\mu{\rm m})$ many times. The absolute value of $\theta_{\rm in}$ is more likely larger than $\theta_{\rm out}$.

in Fig. S5 in the Supplemental Material [31]. As depicted in Fig. 4(b), when θ_1 is in the range of 0 to $\pi/6$, regardless of the value of θ_2 , U_z is always negative; when θ_1 is greater than $\pi/4$, U_z is always positive. Also, it is noted that the geometric constraint ($0 \le \theta_1 + \theta_2 \le \pi/2$), leading to a higher probability of U_z being negative which is 0.61. This indicates that cells near the wall are more likely to be "attracted" as a result of fluid flow, contributing to the occurrence of wall accumulation phenomena.

Besides, when a single cell approaches the wall, disturbances in the surrounding flow field can result in the cell being influenced by nonzero velocity gradients, leading to a cell body rotation near the wall [40]. This effect can be expressed by the following equation:

$$\Omega_z(\theta, h) = -\frac{3p\cos\theta\sin\theta}{64\pi\eta h^3} \left[1 + \frac{(\gamma^2 - 1)}{2(\gamma^2 + 1)} (1 + \sin^2\theta) \right],$$
(3)

where γ is the aspect ratio of the dipole (1.414 for p_1 and 1/1.414 for p_2). Due to the linearity of the low Reynolds number Stokes flow [30], we treat this rotational influence on θ_1 and θ_2 separately. Through calculations, we find that for $0 < \theta_1 < \pi/2$, Ω_1 is always negative, leading θ_1 to decrease, and for $0 < \theta_2 < \pi/2$, Ω_2 is positive, leading θ_2 to increase.

Due to the limitation of our visualization tool, θ_1 cannot be measured directly from the experiment, however, θ_2 can be resolved from the swimming trajectory. To best see this result, we investigate the cell swimming trajectories at different heights, $h = 20 \,\mu\text{m}$ and $h = 50 \,\mu\text{m}$. As depicted in Fig. 5(a), we define the smaller angle between the swimming trajectory and the xy plane when the cell is approaching the surface as θ_{in} and the same angle when the cell is leaving the surface as $\theta_{\rm out}$. We measure the trajectories of 75 cells near this region and plot the distribution of θ_{in} and θ_{out} in Figs. 5(b) and 5(c). For $h = 20 \,\mu\text{m}$, θ_{in} tends to be biased around the $\pi/3$ and $\theta_{\rm out}$ around the $\pi/6$, however, for $h=50\,\mu{\rm m}$, the distribution is less biased. With our 3D real-time tracking technique, the swimming trajectory of a typical cell (starting at $h = 20 \,\mu\text{m}$) is shown in Fig. 5(d). The result aligns with past research that when C. reinhardtii swims toward a wall, it will tend to reorient perpendicular to the wall [40]. When contacting with the solid surface, C. reinhardtii scatters at a smaller angle, leading to the differences between the distributions of θ_{in} and θ_{out} .

Convection-diffusion model for cell distribution. The double force dipole model well explains the mechanism for *C. reinhardtii* being attracted by solid surface. With this result, we further investigate the cell distribution at the steady state. As it is previously discussed, the cell distribution in the observation chamber is uniform right after the suspension is

injected and evolves to the steady state when more cells are located near the surfaces (Fig. 2). We believe such an equilibrium state is the result of balanced convection and diffusion, which is illustrated with the following equation:

$$\frac{\partial}{\partial h}(NU_z) = D\frac{\partial^2 N}{\partial h^2}.$$
 (4)

Here, D is the diffusion coefficient of the cell. As mentioned earlier, we know that θ_1 and θ_2 tend to become 0 and $\pi/2$ near the wall. Thus, we further simplify the velocity expression in Eq. (5) to

$$U(h) = -\frac{1.5p_1}{64\pi nh^2}. (5)$$

Finally, by solving Eq. (4), we obtain the expression for the distribution of cell density with respect to height:

$$\frac{N(h)}{N_0} = \exp\left[L_0\left(\frac{1}{h} + \frac{1}{H-h}\right)\right],\tag{6}$$

where N_0 is related to the number of cells in the system, and $L_0 \approx 23 \,\mu\text{m}$ represents the length scale of the hydrodynamic interaction.

We estimate the force dipole moment generated by *C. reinhardtii* during swimming using the following equation: $p = 64\pi \eta DL/3$; under conditions of water at 20 °C, the diffusion coefficient of cells is approximated to be the same as that of particles with a diameter of 10 μ m. The estimated result obtained was $p \approx 12$ pN μ m, which is close to and slightly smaller than the value estimated through previous theoretical approaches $p \approx 100$ pN μ m. This is possibly due to the periodic swimming behavior of *C. reinhardtii*, and the force

dipole moment estimated from the experimental data is the average over one period, which is naturally smaller than the maximum value.

Conclusions. In this work, we investigate the accumulation phenomenon of *C. reinhardtii* near solid-liquid interface. By tracking individual cells, we find a similar "hopping" trajectory of C. reinhardtii near surfaces as previously reported by Buchner et al. [28]. We propose a double-perpendicularforce dipole model which is different from Klindt et al.'s hypothesis [36] to explain the hydrodynamic interaction between the boundary and the cell. C. reinhardtii, the well-known puller cell, may exert a stronger pusher-type interaction with the ambient fluid, leading to surface accumulation. A convection-diffusion model is developed to explain the distribution of cells in the observation chamber at the steady state. Nonetheless, a closer examination of the cilia motion is missing in our work and the rotational motion along the axis of swimming cannot be measured due to the limitation of our experimental system. Additionally, the dipole moment used in the hypothesis is a rough estimation; more detailed experimental and theoretical studies are needed. In all, we propose a perspective on understanding the swimming behavior of C. reinhardtii near the solid surface and a model for the cell accumulation phenomenon.

Acknowledgments. We thank Dr. Li Zeng for kindly gifting us the cells. We thank Hepeng Zhang and Shuo Guo for the comments and discussions on the paper content. Our work is funded by National Natural Science Foundation of China (NSFC), Grant No. 12202275 and Science and Technology Commission of Shanghai Municipality (STCSM), Grant No. 22YF1419800.

- [1] L. Turner, W. S. Ryu, and H. C. Berg, Real-time imaging of fluorescent flagellar filaments, J. Bacteriol. **182**, 2793 (2000).
- [2] A. Persat, C. D. Nadell, M. K. Kim, F. Ingremeau, A. Siryaporn, K. Drescher, N. S. Wingreen, B. L. Bassler, Z. Gitai, and H. A. Stone, The mechanical world of bacteria, Cell 161, 988 (2015).
- [3] J. S. Guasto, K. A. Johnson, and J. P. Gollub, Oscillatory flows induced by microorganisms swimming in two dimensions, Phys. Rev. Lett. **105**, 168102 (2010).
- [4] E. Lauga, Bacterial hydrodynamics, Annu. Rev. Fluid Mech. 48, 105 (2016).
- [5] T. D. Montenegro-Johnson, D. A. Gagnon, P. E. Arratia, and E. Lauga, Flow analysis of the low reynolds number swimmer *C. elegans*, Phys. Rev. Fluids 1, 053202 (2016).
- [6] G. Juarez, K. Lu, J. Sznitman, and P. E. Arratia, Motility of small nematodes in wet granular media, Europhys. Lett. 92, 44002 (2010).
- [7] E. M. Purcell, Life at low Reynolds number, Am. J. Phys. 45, 3 (1977).
- [8] P. E. Arratia, Life in complex fluids: Swimming in polymers, Phys. Rev. Fluids 7, 110515 (2022).
- [9] K. Drescher, R. E. Goldstein, N. Michel, M. Polin, and I. Tuval, Direct measurement of the flow field around swimming microorganisms, Phys. Rev. Lett. 105, 168101 (2010).
- [10] L. Zhu, E. Lauga, and L. Brandt, Self-propulsion in viscoelastic fluids: Pushers vs. pullers, Phys. Fluids 24, 051902 (2012).

- [11] K. Drescher, J. Dunkel, L. H. Cisneros, S. Ganguly, and R. E. Goldstein, Fluid dynamics and noise in bacterial cell–cell and cell–surface scattering, Proc. Natl. Acad. Sci. USA 108, 10940 (2011).
- [12] C. Fei, S. Mao, J. Yan, R. Alert, H. A. Stone, B. L. Bassler, N. S. Wingreen, and A. Košmrlj, Nonuniform growth and surface friction determine bacterial biofilm morphology on soft substrates, Proc. Natl. Acad. Sci. USA 117, 7622 (2020).
- [13] M. M. Santore, Interplay of physico-chemical and mechanical bacteria-surface interactions with transport processes controls early biofilm growth: A review, Adv. Colloid Interface Sci. 304, 102665 (2022).
- [14] K. T. Hughes and H. C. Berg, The bacterium has landed, Science 358, 446 (2017).
- [15] S. Peng, J. J. Li, W. Song, Y. Li, L. Zeng, Q. Liang, X. Wen, H. Shang, K. Liu, P. Peng, W. Xue, B. Zou, L. Yang, J. Liang, Z. Zhang, S. Guo, T. Chen, W. Li, M. Jin, X.-B. Xing *et al.*, CRB1-associated retinal degeneration is dependent on bacterial translocation from the gut, Cell 187, 1387 (2024).
- [16] D. Scheidweiler, A. D. Bordoloi, W. Jiao, V. Sentchilo, M. Bollani, A. Chhun, P. Engel, and P. D. Anna, Spatial structure, chemotaxis and quorum sensing shape bacterial biomass accumulation in complex porous media, Nat. Commun. 15, 191 (2024).

- [17] W. Chen, N. Mani, H. Karani, H. Li, S. Mani, and J. X. Tang, Confinement discerns swarmers from planktonic bacteria, eLife 10, e64176 (2021).
- [18] X. Chen, X. Dong, A. Be'er, H. L. Swinney, and H. P. Zhang, Scale-invariant correlations in dynamic bacterial clusters, Phys. Rev. Lett. 108, 148101 (2012).
- [19] V. Kantsler, J. Dunkel, M. Polin, and R. E. Goldstein, Ciliary contact interactions dominate surface scattering of swimming eukaryotes, Proc. Natl. Acad. Sci. USA 110, 1187 (2013).
- [20] E. Lushi, V. Kantsler, and R. E. Goldstein, Scattering of biflagellate microswimmers from surfaces, Phys. Rev. E 96, 023102 (2017).
- [21] J. Yuan, D. M. Raizen, and H. H. Bau, A hydrodynamic mechanism for attraction of undulatory microswimmers to surfaces (bordertaxis), J. R. Soc. Interface 12, 20150227 (2015).
- [22] D. Giacché, T. Ishikawa, and T. Yamaguchi, Hydrodynamic entrapment of bacteria swimming near a solid surface, Phys. Rev. E 82, 056309 (2010).
- [23] D. Pimponi, M. Chinappi, P. Gualtieri, and C. M. Casciola, Hydrodynamics of flagellated microswimmers near free-slip interfaces, J. Fluid Mech. 789, 514 (2016).
- [24] R. Di Leonardo, D. Dell'Arciprete, L. Angelani, and V. Iebba, Swimming with an image, Phys. Rev. Lett. 106, 038101 (2011).
- [25] C. N. Dominick and X.-L. Wu, Rotating bacteria on solid surfaces without tethering, Biophys. J. 115, 588 (2018).
- [26] G. Li and J. X. Tang, Accumulation of microswimmers near a surface mediated by collision and rotational brownian motion, Phys. Rev. Lett. 103, 078101 (2009).
- [27] J. Elgeti, U. B. Kaupp, and G. Gompper, Hydrodynamics of sperm cells near surfaces, Biophys. J. 99, 1018 (2010).
- [28] A.-J. Buchner, K. Muller, J. Mehmood, and D. Tam, Hopping trajectories due to long-range interactions determine surface accumulation of microalgae, Proc. Natl. Acad. Sci. USA 118, e2102095118 (2021).
- [29] L. Zeng, W. Jiang, and T. J. Pedley, Sharp turns and gyrotaxis modulate surface accumulation of microorganisms, Proc. Natl. Acad. Sci. USA 119, e2206738119 (2022).
- [30] A. P. Berke, L. Turner, H. C. Berg, and E. Lauga, Hydrodynamic attraction of swimming microorganisms by surfaces, Phys. Rev. Lett. 101, 038102 (2008).
- [31] See Supplemental Material at http://link.aps.org/supplemental/

- 10.1103/PhysRevE.111.L052401 for data from cell swimming experiments and derivation about convection-diffusion equation
- [32] F. J. Schwarzendahl and M. G. Mazza, Maximum in density heterogeneities of active swimmers, Soft Matter 14, 4666 (2018).
- [33] A. Baskaran and M. C. Marchetti, Statistical mechanics and hydrodynamics of bacterial suspensions, Proc. Natl. Acad. Sci. USA 106, 15567 (2009).
- [34] A. Ahmadzadegan, S. Wang, P. P. Vlachos, and A. M. Ardekani, Hydrodynamic attraction of bacteria to gas and liquid interfaces, Phys. Rev. E **100**, 062605 (2019).
- [35] L. Ning, X. Lou, Q. Ma, Y. Yang, N. Luo, K. Chen, F. Meng, X. Zhou, M. Yang, and Y. Peng, Hydrodynamics-induced long-range attraction between plates in bacterial suspensions, Phys. Rev. Lett. **131**, 158301 (2023).
- [36] G. S. Klindt and B. M. Friedrich, Flagellar swimmers oscillate between pusher- and puller-type swimming, Phys. Rev. E 92, 063019 (2015).
- [37] T. Ostapenko, F. J. Schwarzendahl, T. J. Böddeker, C. T. Kreis, J. Cammann, M. G. Mazza, and O. Bäumchen, Curvatureguided motility of microalgae in geometric confinement, Phys. Rev. Lett. 120, 068002 (2018).
- [38] M. Polin, I. Tuval, K. Drescher, J. P. Gollub, and R. E. Goldstein, Chlamydomonas swims with two "gears" in a eukaryotic version of run-and-tumble locomotion, Science 325, 487 (2009).
- [39] K. C. Leptos, M. Chioccioli, S. Furlan, A. I. Pesci, and R. E. Goldstein, Phototaxis of chlamydomonas arises from a tuned adaptive photoresponse shared with multicellular volvocine green algae, Phys. Rev. E 107, 014404 (2023).
- [40] E. Lauga and T. R. Powers, The hydrodynamics of swimming microorganisms, Rep. Prog. Phys. 72, 096601 (2009).
- [41] D. Wei, P. G. Dehnavi, M.-E. Aubin-Tam, and D. Tam, Measurements of the unsteady flow field around beating cilia, J. Fluid Mech. 915, A70 (2021).
- [42] B. M. Friedrich and F. Jülicher, Flagellar synchronization independent of hydrodynamic interactions, Phys. Rev. Lett. 109, 138102 (2012).
- [43] Z. Qu, F. Z. Temel, R. Henderikx, and K. S. Breuer, Changes in the flagellar bundling time account for variations in swimming behavior of flagellated bacteria in viscous media, Proc. Natl. Acad. Sci. USA 115, 1707 (2018).